

Localization and fluctuations in the quantum Hall regime

T. Ando

Institute for Solid State Physics, University of Tokyo, 7-22-1 Roppongi, Minato-ku, Tokyo 106, Japan

(Received 13 August 1993)

A numerical study is performed on the conductance in quantum wires and their junctions in strong magnetic fields. For the lowest Landau level, the energy and system-size dependence of transmission probabilities and their fluctuations is quite universal and characterized by a single parameter within the numerical accuracy. The critical exponent obtained from the width of the transition region between adjacent quantized plateaus is in good agreement with that of localization of bulk Landau states. For the first excited Landau levels, strong mixing between the edge state of the lowest Landau level and bulk states destroys the universality.

I. INTRODUCTION

A key ingredient of the quantum Hall effect is the localization of Landau states in the presence of random potential fluctuations. It has been shown in various different ways that the Hall conductivity is quantized into integer multiples of $-e^2/h$ when states around the Fermi level are all localized. Several reviews have been published already.¹⁻³ In quantum wires, on the other hand, the Hall effect is understood in terms of the transmission probability of edge channels.⁴ In fact, the Hall resistance is quantized whenever backscattering of edge states is negligible. The relationship between these two pictures remains unclear. The purpose of the present paper is to study the conductance and its fluctuation in two-dimensional systems in high magnetic fields based on the edge-current picture and to compare the results with those predicted in the bulk-state picture.

In the picture based on bulk Landau states, the width of the Hall steps, i.e., the region where the Hall conductivity changes from a quantized value to another, is determined by delocalized states existing in the vicinity of the center of each broadened Landau level.^{5,6} In the edge-current picture, on the other hand, the Hall-step width is determined by backscattering through mixing with bulk states. There have already been various theoretical investigations on such mixing.⁷⁻⁹

The conductance fluctuations are universal in metallic diffusive systems when their size becomes smaller than the phase-coherence length. This has theoretically been shown first by perturbation calculations.¹⁰⁻¹³ Fluctuations in the quantum Hall regime have also been the subject of both theoretical and experimental study. For example, a perturbation calculation, valid only for highly excited Landau levels,¹⁴ and a numerical study¹⁵ have been performed. Effects of a Hall electric field were investigated quite recently.¹⁶ It is known experimentally that fluctuations become appreciable in the transition region between quantized plateaus.^{17,18} Magnetic-field dependence of the correlation field of fluctuations has been studied for diffusive quantum wires in high magnetic fields.¹⁹

In this paper, the scattering probabilities of edge states

are calculated numerically for both two- and four-terminal geometries. It will be shown that the dependence of the Hall-step width on the wire width is determined by the energy dependence of the localization length of bulk Landau states, in agreement with the behavior predicted in the bulk-current picture. The fluctuations and the distribution function of the conductance are calculated in a two-terminal geometry and their universal behavior is demonstrated. The universality prevails also for various transmission probabilities in a four-terminal geometry. In Sec. II a brief discussion is given of the model and the method of calculation. Some examples of numerical results are given for the average conductance and the fluctuation in a two-terminal geometry in Sec. III and in a four-terminal crossed-wire geometry in Sec. IV. Section V deals with a brief summary and discussion. A very preliminary account of a part of the present work has been published elsewhere.^{20,21}

II. MODEL AND METHOD

We consider a two-dimensional (2D) system on a square lattice and introduce effects of scattering through randomness of site energy distributed uniformly with a width corresponding to broadening Γ of the Landau level calculated in the self-consistent Born approximation.^{22,23} A magnetic-field H is included in the form of a Peierls' phase factor in the nearest-neighbor transfer integral. The lattice system with M sites in the y direction, for example, corresponds to a continuum system with width $W=(M+1)a$ for sufficiently large M , where a is the lattice constant.

We consider both two- and four-terminal geometries, schematically illustrated in Fig. 1. For the two-terminal case, a wire with width W in the y direction and length L in the x direction is connected to an infinitely long ideal wire, which is eventually connected to a reservoir. For the four-terminal geometry, we shall consider a junction of two wires with length L and width W . Ideal wires are connected at all ends. In order to calculate transmission probability for the entire energy range of the broadened 2D Landau levels, we shall lower the bottom energy in the ideal wires by ΔE ($\Gamma < \Delta E < \hbar\omega_c - \Gamma$ with

$\omega_c = eH/mc$) as shown in Fig. 1. This is required because without ΔE current-carrying edge channels disappear in ideal wires and the transmission likewise vanishes when the energy is smaller than that of the lowest Landau level.

The transmission probabilities are calculated using the Green-function technique already described.²⁴ The conductance can easily be given by the Büttiker-Landauer formula.²⁵ In the two-terminal case, for example, we have

$$G = \frac{e^2}{\pi\hbar} T, \quad (2.1)$$

with T being the transmission probability, where a small spin splitting is completely neglected. We should make the magnetic flux passing through a unit cell as small as possible in order to avoid peculiarities characteristic of lattice systems.²⁶ Actual numerical calculations are performed for systems with width W lying between $W/l=5$ and 50, where l is the magnetic length given by $l = \sqrt{c\hbar/eH}$. The corresponding number of the lattice sites are listed in Table I. For these parameters, the lattice system can simulate the corresponding continuum system quite well, although there remain some effects due to the nonparabolicity, as will be discussed in the next section.

The transmission probability for a given energy is calculated by averaging over those of typically a few times 10^3 different samples. The broadening of the Landau level is $\Gamma/\hbar\omega_c = 0.2$ and the energy shift is chosen as $\Delta E = \hbar\omega_c/2$. Actual numerical calculations show that a slight change in the choice of the shift causes negligible effects for wires with sufficiently large width. Numerical calculations are performed for $L/W = \frac{1}{2}, 1$, and 2 in the two-terminal case and for $L/W = 3$ in the crossed-wires geometry.

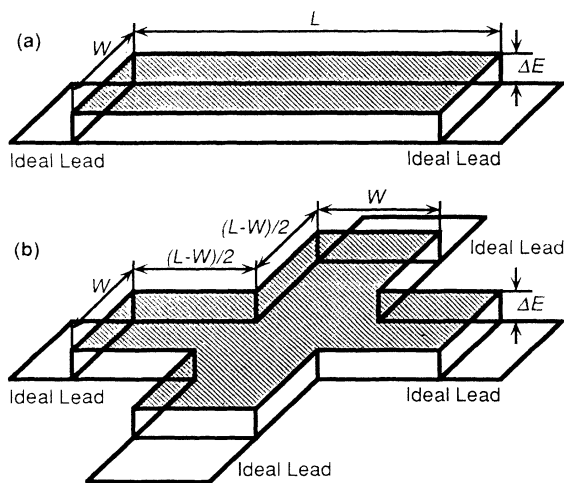


FIG. 1. Schematic illustration of a quantum wire (a) and its crossing (b) with width W and length L . The wire is confined by infinitely high barriers in one direction and connected to an infinitely long ideal wire, which is eventually connected to a reservoir. The bottom energy is raised by ΔE from that in the ideal wire.

TABLE I. Wire width in units of the magnetic length l and the lattice constant a , and corresponding magnetic flux passing through a unit cell in units of the flux quantum $\Phi_0 = ch/e$.

W/l	W/a	a^2H/Φ_0
5.0	8	0.062 17
10.0	16	0.062 17
15.0	24	0.062 17
20.0	40	0.039 79
25.0	56	0.031 72
30.0	80	0.022 38
35.0	100	0.019 50
40.0	128	0.015 54
50.0	200	0.009 95

III. TWO-TERMINAL GEOMETRY

A. Critical exponent of localization

Figure 2 shows an example of the conductance as a function of energy for a typical system with width $W/l=20$ and length $L/l=20$. The conductance vanishes below the energy of the broadened 2D Landau level ($E < \hbar\omega_c/2 - \Gamma$) and becomes $e^2/\pi\hbar$ above $E > \hbar\omega_c/2 + \Gamma$. In the energy range of broadened Landau states, on the other hand, it exhibits a large fluctuation with amplitude of the same order as the conductance and consists of sharp spikes and peaks.

Figure 3 gives some examples of calculated energy dependence of the averaged conductance given by $\langle G \rangle = (e^2/\pi\hbar)\langle T \rangle$ for the lowest Landau level, where $\langle \dots \rangle$ denotes a sample average. The dotted lines represent the transmission probability for square systems with $L/W = 1$ in the absence of randomness. Except for the narrow system with $W/l=5$, it is essentially a step

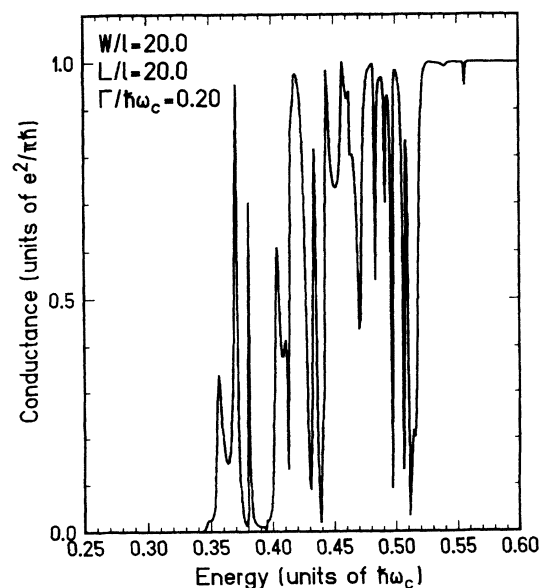


FIG. 2. An example of calculated conductance of the lowest Landau level as a function of energy. $W/l = L/l = 20$.

function rising at the energy of the Landau level in two dimensions, which is slightly smaller than $\hbar\omega_c/2$ because of the small nonparabolicity present in the lattice model. The transition probability in the presence of randomness exhibits a much slower increase and the energy dependence becomes steeper with an increase of the system size.

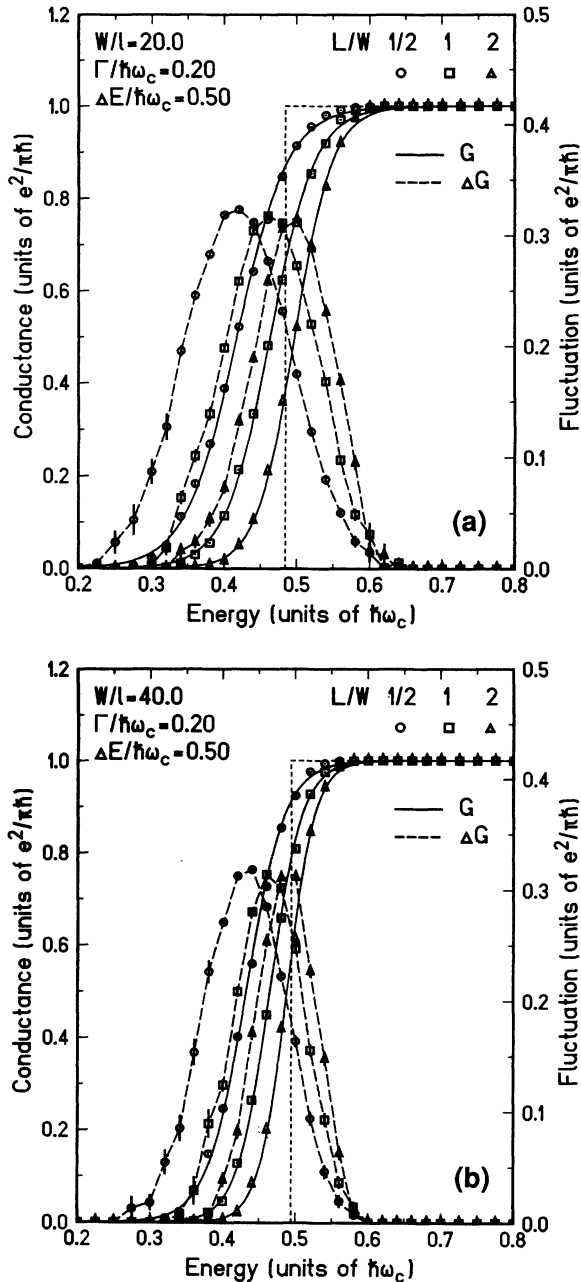


FIG. 3. Calculated conductance and its fluctuation (the open symbol) as a function of energy for the lowest Landau level. The circles denote the results for a short rectangular system ($L/W=1/2$), squares those for a square ($L/W=1$), and triangles those for a long rectangular system ($L/W=2$). The dotted line represents the conductance in the absence of randomness. The solid lines represent Eq. (3.1) and the dashed lines are guides to the eye. (a) $W/l=20$ and (b) $W/l=40$.

In order to deduce the effective energy width over which the transmission probability increases from zero to unity, we fit the results to the function

$$\langle T(E) \rangle = \frac{1}{\exp[\beta(E - E_{th})] + 1}. \quad (3.1)$$

The parameter β or $\Gamma(d\langle T \rangle/dE)_{\max}$ represents the inverse of the effective energy width and E_{th} the effective threshold energy. The fitted results are shown by solid lines in Fig. 3. Although the fitting is not perfect, particularly in the region where $\langle T \rangle \sim 0$ and 1, this procedure is expected to be sufficient in determining the effective width and threshold.

Figure 4 gives the steepness parameter as a function of the width in logarithmic scales. It is clear that the results can be fitted to a straight line, except those for $W/l=5$, showing that $\Gamma(d\langle T \rangle/dE)_{\max} \propto W^{1/s}$. The exponent is almost independent of the form of the system and is obtained as $s=2.2 \pm 0.1$.

Figure 3 shows that the threshold energy for square systems is slightly lower than the Landau-level energy in two dimensions. This is mainly due to a quantum-mechanical level repulsion effect caused by interactions among different Landau levels. The threshold energy becomes larger with increasing L for a given W , and that for systems with different L/W 's becomes closer with increasing system size. Figure 4 also shows the difference

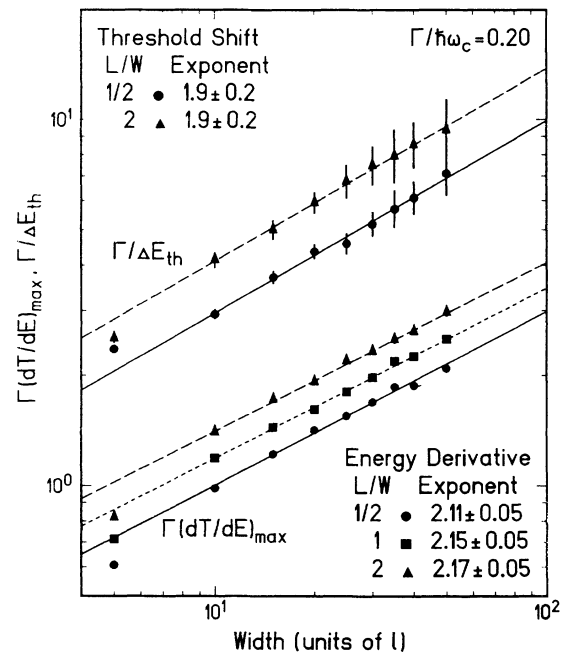


FIG. 4. Log-log plot of the maximum energy derivative of the two-terminal conductance as a function of the wire width. The straight lines represent $\Gamma(d\langle T \rangle/dE)_{\max} \propto W^{1/s}$ with exponents s listed at the bottom-right corner. The dots denoted as $\Gamma/\Delta E_{th}$ represent the threshold energy difference between $L/W=1$ and $1/2$, and the squares the difference between $L/W=2$ and 1. The exponents s' defined by $\Delta E_{th} \propto W^{-1/s'}$ are listed at the top-left corner.

in the threshold energy $\Delta E_{\text{th}}^{(2)} = E_{\text{th}}^{L/W=2} - E_{\text{th}}^{L/W=1}$ and $\Delta E_{\text{th}}^{(1/2)} = E_{\text{th}}^{L/W=1} - E_{\text{th}}^{L/W=1/2}$. Although statistical errors are much larger, ΔE_{th} is also fitted to a power-law dependence, $\Delta E_{\text{th}} \propto W^{-1/s'}$. The resulting $s' = 1.9 \pm 0.2$ agrees with s within statistical errors.

Numerical Thouless-number study of localization for Landau levels has shown that states are all localized except those lying in the vicinity of the center in two dimensions.^{27,28} The critical exponent s , defined by $\alpha \propto |E|^s$, with α being the inverse localization length and the energy origin chosen at the center of the broadened Landau level, was obtained as $s \sim 2$ for the lowest Landau level. This result was consistent with that obtained in a lattice model,²⁹ and was also later confirmed by finite-size scaling calculations.^{30,31} More recent finite-size scaling calculations within a random-matrix model³² gave the exponent $s \approx 2.3$. A numerical study on the topological winding number related to the Hall conductivity also gave a similar result.³³

Let $E_- (<0)$ represent the energy below the Landau level where the transmission becomes appreciable and $E_+ (>0)$ denote the energy above which the backscattering becomes negligible. For sufficiently large systems where localization length α^{-1} is the only relevant length scale, these energies are determined by the condition $h_{\pm}[\alpha(E_{\pm})L, \alpha(E_{\pm})W] = 1$ with h_{\pm} as a certain function. This leads to $E_{\pm}/\Gamma = \pm C_{\pm}(W/l)^{-1/s}$ for $\alpha(E) \propto |E|^s$ with C_{\pm} as an appropriate constant depending only on the ratio L/W . Therefore, the width of the energy region over which the transmission probability varies from zero to unity is given by $E_+ - E_- \propto W^{-1/s}$, i.e., $\Gamma(d\langle T \rangle/dE)_{\text{max}} \propto (E_+ - E_-)^{-1} \propto W^{1/s}$. This means that the exponents s and s' obtained above are both equal to that for the inverse localization length of bulk 2D Landau states.

In more physical but less accurate terms, E_- is expected to be determined by the condition $\alpha(E_-)L \sim 1$ because the transmission is possible only through bulk extended states for energy below the bulk Landau level. Similarly, E_+ is expected to be determined by the condition $\alpha(E_+)W \sim 1$ because the backscattering is possible only through the bulk states. This argument immediately leads to the same conclusion mentioned above. It also suggests a possibility that the exponent s obtained above is slightly underestimated. In fact, an effective width W_{eff} is smaller than W by an amount corresponding to the extent of the wave function of edge states and the deviation of W_{eff} from W becomes more important for systems with smaller W . This will lead to a weaker dependence of $\Gamma(d\langle T \rangle/dE)_{\text{max}}$ on W_{eff} than on W , and a slightly larger value for the exponent s . It is difficult, however, to estimate the amount of such a deviation because of the ambiguity in the choice of W_{eff} .

B. Fluctuations

Figure 3 contains also the conductance fluctuation $\sqrt{\langle (G - \langle G \rangle)^2 \rangle}$. The fluctuation takes a maximum almost independent of the form of the system, i.e., L/W , around the energy where the conductance is half of the

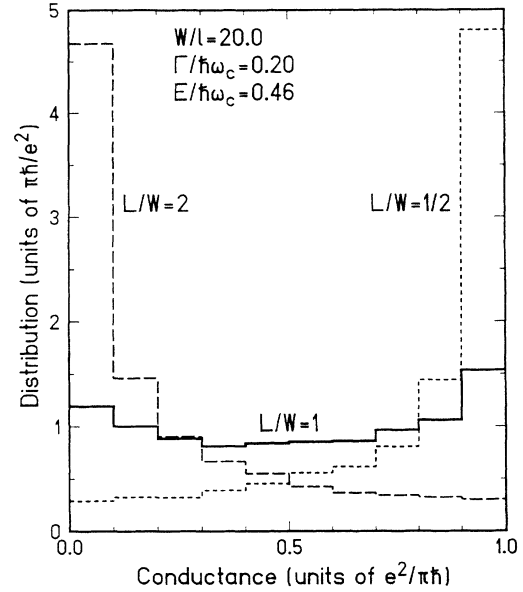


FIG. 5. Examples of the distribution function of the conductance for wires with width $W/l = 20$. For a square system with L/W , the average conductance is nearly $0.5e^2/\pi\hbar$ and the fluctuation takes a maximum.

quantized value $e^2/\pi\hbar$ and exhibits the steepest energy dependence. The maximum fluctuation is nearly independent of the system size and is given by a value very close to $\Delta G = 0.31e^2/\pi\hbar$ obtained by perturbation calculations for 2D metallic systems in weak magnetic fields.¹⁰⁻¹³ The fluctuations appear only in the energy range where the conductance deviates from quantized values. This is in good agreement with the experimental

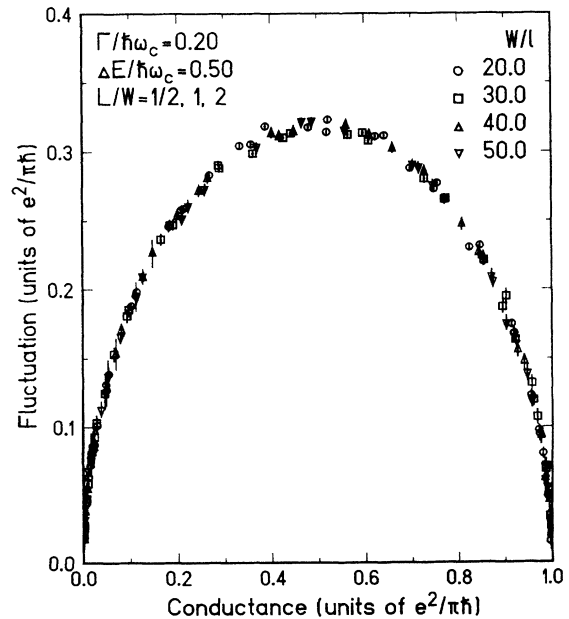


FIG. 6. Calculated fluctuations as a function of the average conductance for the lowest Landau level for wires with different width and length.

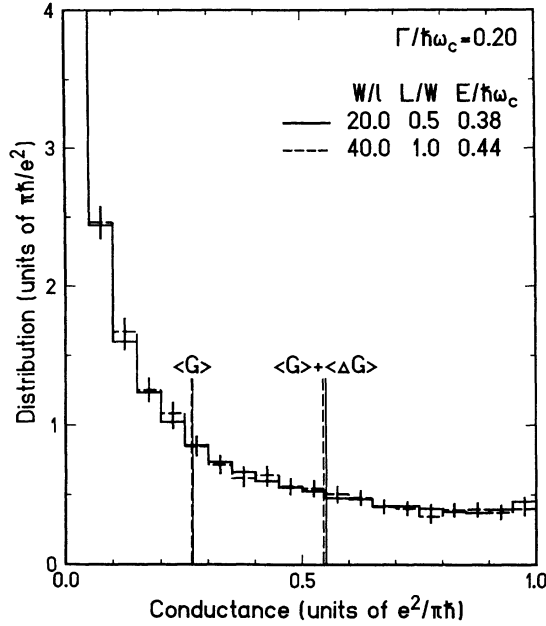


FIG. 7. Distribution function of the conductance for systems with nearly the same average conductance. Solid line: $W/l=20$, $L/W=1/2$, and $E/\hbar\omega_c=0.38$. Dashed line: $W/l=40$, $L/W=1$, and $E/\hbar\omega_c=0.44$.

finding that they become appreciable in the transition region between quantized plateaus.^{17,18}

This maximum fluctuation is slightly larger than $\sqrt{1/12}=0.29$ in units of $e^2/\pi\hbar$ obtained for the uniform distribution in which the conductance distributes uniformly between 0 and $e^2/\pi\hbar$. In fact, the distribution

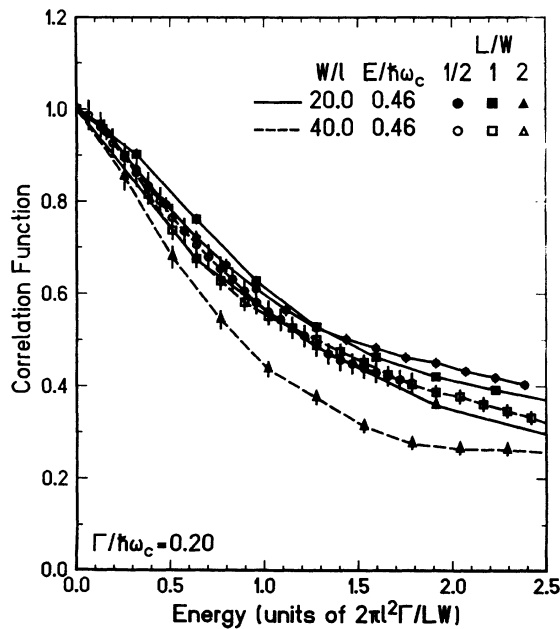


FIG. 8. Examples of energy correlation functions of the conductance. Solid lines and open symbols: $W/l=20$ and $E/\hbar\omega_c=0.46$. Dashed lines and closed symbols: $W/l=40$ and $E/\hbar\omega_c=0.46$.

function has larger value near 0 and $e^2/\pi\hbar$ than near $(1/2)e^2/\pi\hbar$ at the maximum fluctuation where the average conductance is $(1/2)e^2/\pi\hbar$. Some examples of the distribution functions are given in Fig. 5. When $\langle G \rangle$ is smaller than $(1/2)e^2/\pi\hbar$, the distribution function has a large peak at $G=0$ and a long tail for larger G . When $\langle G \rangle$ is larger than $(1/2)e^2/\pi\hbar$, on the other hand, it has a larger peak at $G=e^2/\pi\hbar$ and a long tail for smaller G .

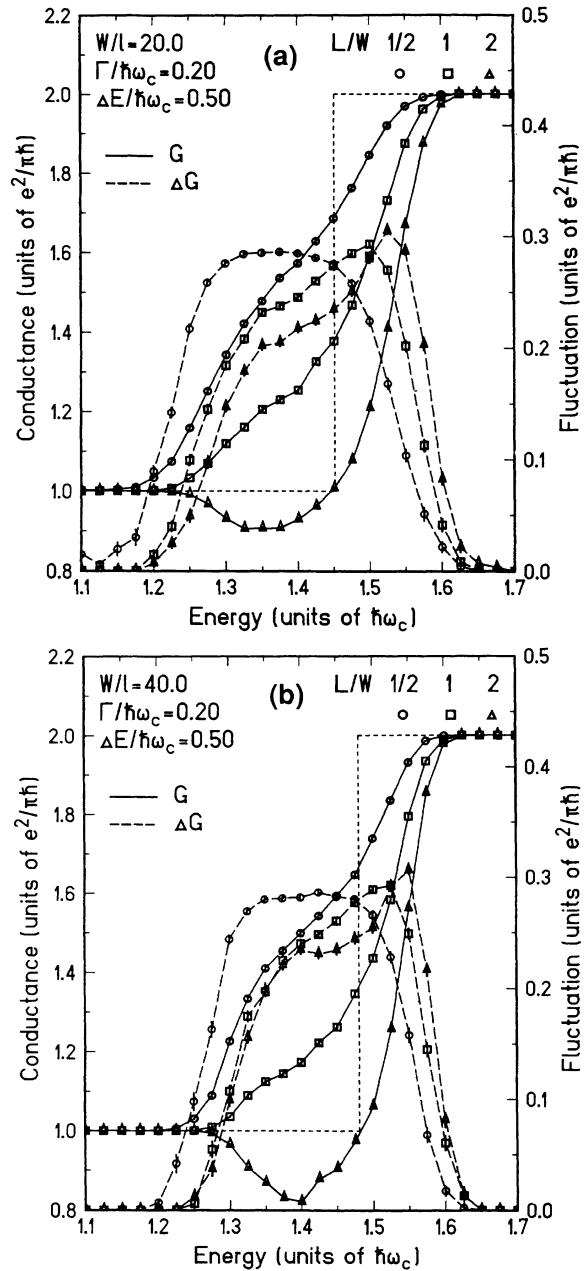


FIG. 9. Calculated conductance and its fluctuation as a function of energy for the first excited Landau level. The circles denote the results for a short rectangular system ($L/W=1/2$), squares those for a square, and triangles those for a long rectangular system ($L/W=2$). The dotted line represents the conductance in the absence of randomness. The solid and dashed lines are guides to the eye. (a) $W/l=20$ and (b) $W/l=40$.

Figure 3 suggests the presence of a universal relation between the average conductance and fluctuation. Figure 6 gives the fluctuation as a function of the average conductance for wires with width $W/l=20, 30, 40,$ and 50 and length $L/W=\frac{1}{2}, 1,$ and 2 . This shows that the fluctuation is determined within the numerical accuracy by the average conductance alone. The universality can also be seen from the distribution function of the conductance given in Fig. 7, where the distribution function is plotted for two cases corresponding to different system forms and energies but having similar $\langle G \rangle$ and ΔG . A correlation between the diagonal conductivity σ_{xx} and the fluctuation of the Hall conductivity σ_{xy} in 2D systems on a torus has been suggested by Aoki.³⁴

An important quantity related to fluctuations is the correlation between different energies. In metallic diffusive systems, the correlation energy E_c is given by the Thouless energy $\hbar D/LW$ with D being the diffusion coefficient.¹⁰⁻¹³ In the present system, the diffusion coefficient is roughly given by^{22,23} $2\pi l^2/\tau$ with $\tau \sim \hbar/\Gamma$ and the correlation energy is expected to be

$$E_c \sim \Gamma \frac{2\pi l^2}{LW}. \quad (3.2)$$

Figure 8 shows examples of the energy correlation function

$$F(\epsilon) = \langle G(E)G(E+\epsilon) \rangle \langle G(E)^2 \rangle^{-1}, \quad (3.3)$$

for wires with width $W/l=20$ and 40 , which demonstrates the correctness of Eq. (3.2). We can expect safely, without explicit calculations, that the correlation magnetic field is also given by that estimated in a manner similar to that in metallic diffusive systems.¹⁴ There seems to be a slight deviation of E_c from that given by Eq. (3.2) for the long system with $L/W=2$ and

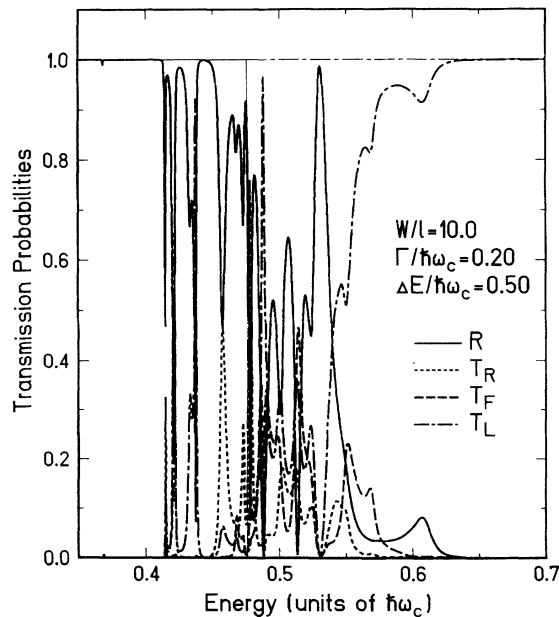


FIG. 10. Calculated reflection and transmission probabilities at a wire junction with width $W/l=10$.

$W/l=40$. This may possibly be due to a precursor of the localization effect because the transmission itself is already quite small ($\langle T \rangle \sim 0.1$).

C. Excited Landau levels

The situation changes drastically for the first excited Landau level as shown in Fig. 9. In fact, the energy dependence of the conductance itself is quite different from that for the lowest Landau level and varies considerably with the change in the form of the system. For systems with a long rectangular form ($L/W=2$), the

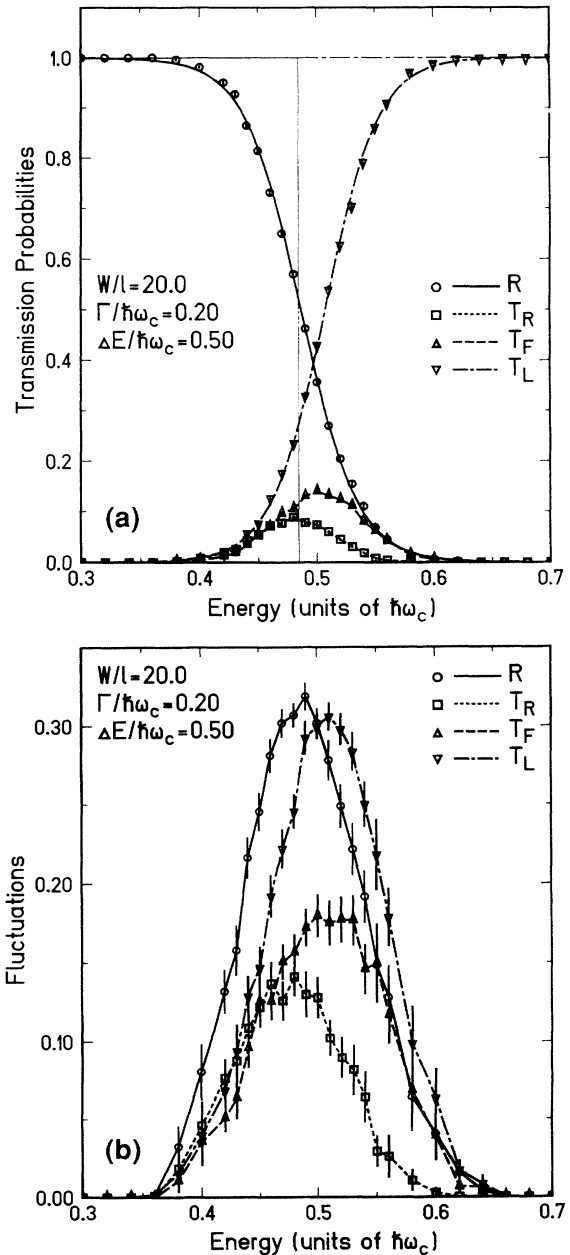


FIG. 11. Averaged reflection and transmission probabilities (a) and their fluctuations (b) at wire junctions with width $W/l=20$. The lines for $\langle R \rangle$ and $\langle T_L \rangle$ represent Eq. (4.1) fitted to the results.

average conductance first decreases slightly from $e^2/\pi\hbar$ before reaching $2e^2/\pi\hbar$ with increasing energy. This reduction is stronger with increasing system size.

The reduction of the two-terminal conductance at the energy of bulk Landau states has already been obtained analytically in the self-consistent Born approximation³⁵ and also numerically,^{36,15} and is a result of a strong mixing of the edge state associated with the lowest Landau level with the first excited bulk Landau states. The mixing makes it difficult to extract information on the first excited Landau level alone and even modifies the nature

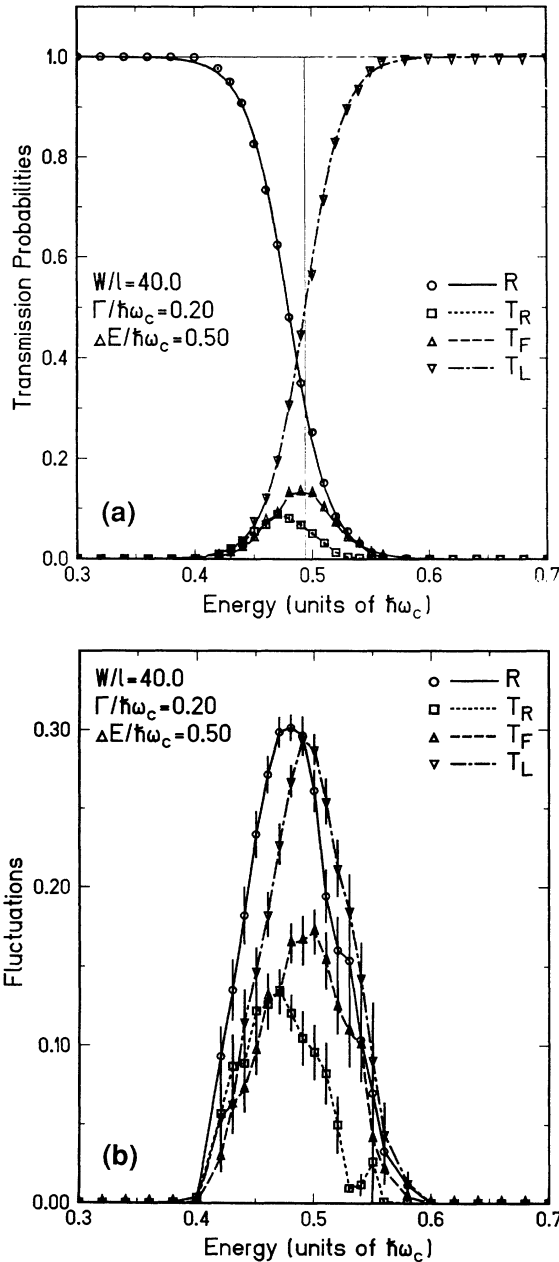


FIG. 12. Averaged reflection and transmission probabilities (a) and their fluctuations (b) at wire junctions with width $W/l=40$. The lines for $\langle R \rangle$ and $\langle T_L \rangle$ represent Eq. (4.1) fitted to the results.

of the Landau states as well as the edge state.²⁹ In spite of such complications, however, the facts remain that the fluctuation becomes appreciable in the energy range where the conductance deviates from quantized values and that the maximum in the fluctuation moves to higher energy with increasing system length L for a fixed width W . The maximum fluctuation for the long rectangular system ($L/W=2$) is approximately the same as that for the lowest Landau level.

In actual quantum wires, fabricated at a GaAs/Al_xGa_{1-x}As heterostructure, for example, the confinement is given by a slowly varying potential rather than the abrupt infinite barrier as assumed here. The strength of the confinement may depend strongly on how the system is prepared. For a very slowly varying confining potential, a mixing among edge states and between edge and bulk states is expected to be negligible because of a small spatial overlap of the wave functions.³⁷⁻⁴⁰ Therefore, the edge states associated with the lowest Landau level is hardly coupled with bulk states of the first excited Landau level and the energy dependence of the conductance becomes essentially the same as that for the lowest Landau level. Further, a self-consistency in the confinement potential and the electron-density distribution is essential.⁴¹⁻⁴³ As a consequence, the edge state associated with the lowest Landau level may lose its character when the Fermi level lies at the first excited Landau level.

IV. CROSSED-WIRES GEOMETRY

Figure 10 shows an example of calculated reflection (R) and transmission probabilities, turning right (T_R), turn-

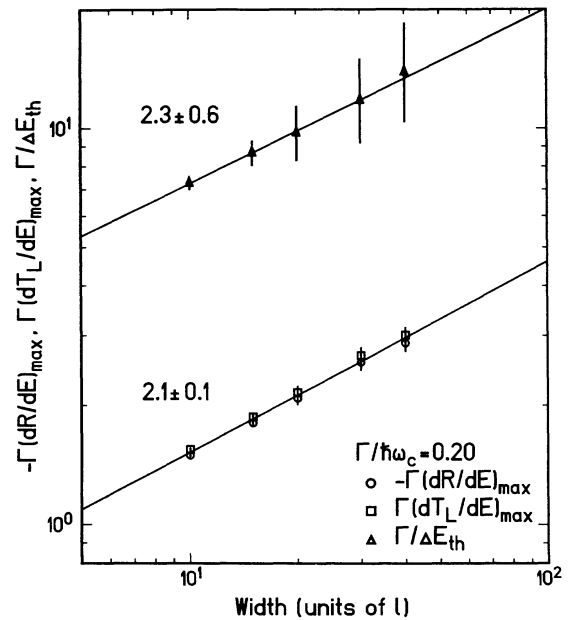


FIG. 13. Log-log plot of the maximum derivatives of the averaged reflection $\langle R \rangle$ and transmission probability $\langle T_L \rangle$, and the inverse of the difference of the threshold energy for $\langle R \rangle$ as a function of the wire width for crossed-quantum wires. The straight lines represent $W^{1/s}$ with critical exponent s listed.

ing left (T_L), and going straight (T_F), as a function of energy for the lowest Landau level and for width $W/L=10$. They exhibit large fluctuations consisting of sharp peaks and dips in the energy range of the broadened 2D Landau level.

Using similar results for different samples, we can calculate their averages $\langle R \rangle$, etc., fluctuations $\sqrt{\langle (R - \langle R \rangle)^2 \rangle}$, etc., and also the correlation functions such as $\langle (R - \langle R \rangle)(T_L - \langle T_L \rangle) \rangle$, etc. Figure 11 shows an example for $W/l=20$ and Fig. 12 that for $W/l=40$.

With the increase of the wire width, the transition region, where $\langle R \rangle$ and $\langle T_L \rangle$ change between zero and

unity and where $\langle T_R \rangle$ and $\langle T_F \rangle$ are nonzero, becomes narrower. The effective width of this transition region can be deduced by fitting the results to

$$\langle R \rangle = \frac{1}{\exp[-\beta_R(E - E_{th}^R)] + 1}, \quad (4.1)$$

$$\langle T_L \rangle = \frac{1}{\exp[\beta_T(E - E_{th}^T)] + 1},$$

with two parameters β_R and E_{th}^R for $\langle R \rangle$ and β_T and E_{th}^T for $\langle T_L \rangle$. The fitted results are shown by solid lines for

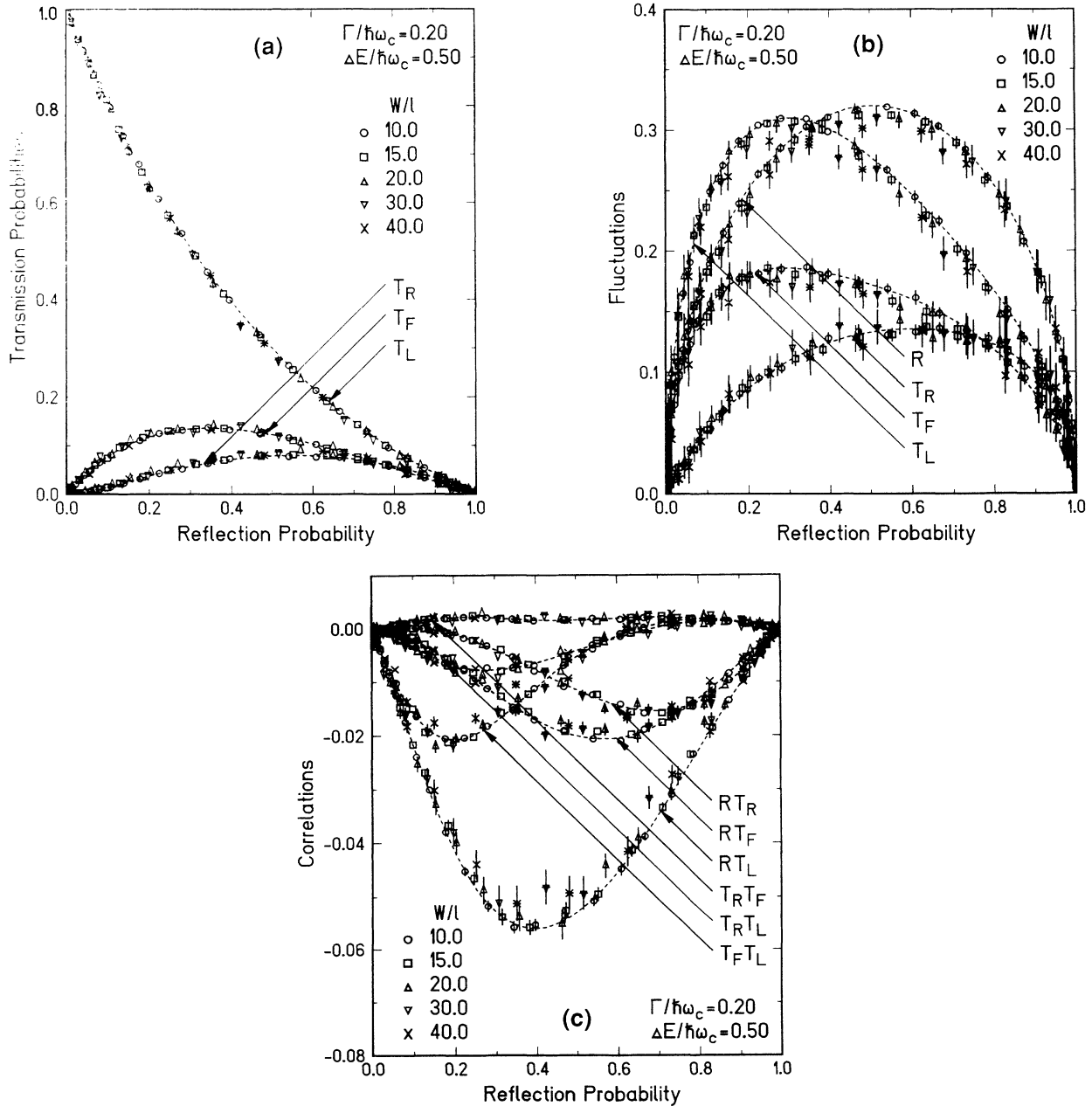


FIG. 14. Average transmission probabilities (a), fluctuations of transmission and reflection probabilities (b), and correlations among transmission and reflection probabilities (c) vs average reflection probability at wire junctions with different width. The dotted lines are guides to the eye.

$\langle R \rangle$ and by dot-dashed lines for $\langle T_L \rangle$ in Figs. 11 and 12. The fitting is not perfect, but this is again expected to be sufficient in determining the effective width and threshold.

Figure 13 shows the maximum derivative $-\Gamma(d\langle R \rangle/dE)_{\max} \propto \beta_R$ and $\Gamma(d\langle T_L \rangle/dE)_{\max} \propto \beta_T$ as a function of W together with $\Delta E_{\text{th}}^{TR} = E_{\text{th}}^T - E_{\text{th}}^R$. Within the numerical accuracy, the critical exponents obtained for the crossed-wires geometry agree with those obtained for the two-terminal case discussed in the previous section. This is consistent with the fact that $\alpha(E)$ is the only relevant parameter in the present system.

The results for systems with a different size suggest a universality similar to that in the case of the two-terminal geometry. Figure 14(a) gives the average transmission probabilities as a function of the average reflection probabilities for systems with width $W/l = 10, 15, 20, 30,$ and 40 . It is evident that the average transmission probabilities are determined by $\langle R \rangle$ alone within the present numerical accuracy. The universality prevails also for the fluctuations and correlation functions as is shown in Figs. 14(b) and 14(c).

Experimentally, the transport coefficients in quantum wires are usually measured in a crossed-wires geometry and various interesting phenomena arising from ballistic transmission across wire junctions have been observed. One of the most typical examples is the anomalies in the low-field Hall effect, such as quenching and the last plateau.⁴⁴ These anomalies are believed to arise from the presence of a large rounding of the corner of the junction. Such a rounding certainly affects the present results on the transmission probabilities, but is expected not to alter the conclusion about the ‘‘universality’’ that $\alpha(E)$ is the only relevant parameter. The presence of a rounding may introduce another length scale such as a radius of curvature and makes the analysis much more complicated. This problem is left for a future study.

V. SUMMARY AND DISCUSSION

We have studied the conductance and its fluctuations in quantum wires in the quantum Hall regime numerically. Within the numerical accuracy, the conductance for the lowest Landau level is characterized by a single parameter $\alpha(E)$ for both two-terminal and crossed-wires geometry, where $\alpha(E)$ is the inverse localization length of

the 2D Landau level. Consequently, for a fixed form of the system, the distribution function for the conductance is determined by a single parameter such as the average conductance. This is quite analogous to the results obtained by a previous numerical study that there is a universal relationship between σ_{xx} and σ_{xy} independent of the system size within the statistical errors.⁴⁵ For the first excited Landau level, a strong mixing of edge states associated with the lowest Landau level and bulk states modifies the nature of these states, which seems to destroy the universal behavior.

A direct comparison of the present results with fluctuations observed in actual systems with size L larger than the phase coherence L_ϕ may require some caution. For $L, W \gg L_\phi$ the system is usually separated into regions with size L_ϕ independent of each other. In this case, however, clear system boundaries and edge states are not present in each region, while the present system has a real boundary potential giving rise to current-carrying edge states.

The critical exponent for the localization of 2D lowest Landau states is obtained as 2.2 ± 0.1 . This is consistent with that of almost all the existing theories, either numerical^{27–33} or analytical,⁴⁶ because actual errors are likely to be larger than $\sim \pm 0.1$ estimated statistically. Koch *et al.* investigated the wire-width dependence of the width of the transition region between quantized Hall plateaus in narrow wires at low temperatures and deduced a critical exponent ($s \sim 2.3$) for the localization length of bulk Landau states.⁴⁷ The present result justifies this experimental procedure of determining s , although the lateral confining potential in actual GaAs/Al_xGa_{1-x}As heterostructures is believed to be slowly varying rather than the abrupt potential assumed above.

ACKNOWLEDGMENTS

This work was supported in part by the Industry-University Joint Research Program ‘‘Mesoscopic Electronics’’ and by the grants-in-aid for Scientific Research on Priority Areas, ‘‘Electron Wave Interference Effects in Mesoscopic Structures’’ and ‘‘Computational Physics as a New Frontier in Condensed Matter Research,’’ from the Ministry of Education, Science and Culture, Japan.

¹T. Ando, Prog. Theor. Phys. Suppl. **84**, 69 (1985).

²*The Quantum Hall Effect*, edited by R. E. Prange and S. M. Girvin (Springer, New York, 1987).

³H. Aoki, Rep. Prog. Phys. **50**, 655 (1987).

⁴M. Büttiker, Phys. Rev. Lett. **57**, 1761 (1986).

⁵H. P. Wei, D. C. Tsui, M. A. Paalanen, and A. M. M. Pruisken, Phys. Rev. Lett. **61**, 1294 (1988).

⁶J. Wakabayashi, M. Yamane, and S. Kawaji, J. Phys. Soc. Jpn. **58**, 1903 (1989).

⁷T. Ohtsuki and Y. Ono, J. Phys. Soc. Jpn. **58**, 1705 (1989).

⁸Y. Ono, T. Ohtsuki, and B. Kramer, J. Phys. Soc. Jpn. **58**, 956 (1989).

⁹T. Ando, Phys. Rev. B **42**, 5626 (1990).

¹⁰B. L. Altshuler, Pis'ma Zh. Eksp. Teor. Fiz. **41**, 530 (1985) [JETP Lett. **41**, 648 (1985)].

¹¹P. A. Lee and A. D. Stone, Phys. Rev. Lett. **55**, 1622 (1985).

¹²B. L. Altshuler and D. E. Khmel'nitskii, Pis'ma Zh. Eksp. Teor. Fiz. **42**, 291 (1986) [JETP Lett. **42**, 359 (1986)].

¹³P. A. Lee, A. D. Stone, and H. Fukuyama, Phys. Rev. B **35**, 1039 (1987).

¹⁴S.-H. Xiong and A. D. Stone, Phys. Rev. Lett. **68**, 3757 (1992).

¹⁵H. Tamura and T. Ando, Phys. Rev. B **44**, 1792 (1991).

¹⁶D. E. Khmel'nitskii and M. Yosefin, Surf. Sci. (to be published).

¹⁷G. Timp, A. M. Chang, P. Mankiewich, R. Behringer, J. E. Cunningham, T. Y. Chang, and R. E. Howard, Phys. Rev.

- Lett. **59**, 732 (1987).
- ¹⁸A. K. Geim, P. C. Main, P. H. Beton, P. Streda, L. Eaves, C. D. W. Wilkinson, and S. P. Beaumont, Phys. Rev. Lett. **67**, 3014 (1991).
- ¹⁹A. K. Geim, P. C. Main, P. H. Beton, L. Eaves, S. P. Beaumont, and C. D. W. Wilkinson, Phys. Rev. Lett. **69**, 1248 (1992).
- ²⁰T. Ando, J. Phys. Soc. Jpn. **61**, 415 (1992).
- ²¹T. Ando, Physica B **184**, 361 (1993).
- ²²T. Ando and Y. Uemura, J. Phys. Soc. Jpn. **36**, 959 (1974).
- ²³T. Ando, J. Phys. Soc. Jpn. **36**, 1521 (1974); **37**, 622 (1974); **37**, 1233 (1974).
- ²⁴T. Ando, Phys. Rev. B **44**, 8017 (1991).
- ²⁵R. Landauer, IBM J. Res. Dev. **1**, 223 (1957); Philos. Mag. **21**, 863 (1970).
- ²⁶D. R. Hofstadter, Phys. Rev. B **14**, 2239 (1976).
- ²⁷T. Ando, J. Phys. Soc. Jpn. **52**, 1893 (1983); **53**, 310 (1983); **53**, 3126 (1983); Phys. Rev. B **40**, 9965 (1989).
- ²⁸H. Aoki, Surf. Sci. **196**, 107 (1988).
- ²⁹T. Ando, Phys. Rev. B **40**, 5325 (1989).
- ³⁰H. Aoki and T. Ando, Phys. Rev. Lett. **54**, 831 (1985).
- ³¹T. Ando and H. Aoki, J. Phys. Soc. Jpn. **54**, 2238 (1985).
- ³²B. Huckerstein and B. Kramer, Phys. Rev. Lett. **64**, 1437 (1990); Solid State Commun. **71**, 445 (1989).
- ³³Y. Huo and R. N. Bhatt, Phys. Rev. Lett. **68**, 1375 (1992).
- ³⁴H. Aoki, in *High Magnetic Fields in Semiconductor Physics III*, edited by G. Landwehr (Springer, Heidelberg, 1992), p. 17.
- ³⁵H. Bruus and K. Flensberg, J. Phys. Condens. Matter **4**, 9131 (1992).
- ³⁶J. M. Kinaret and P. L. Lee, Phys. Rev. B **43**, 3847 (1991).
- ³⁷H. Hirai, S. Komiyama, S. Hiyamizu, and S. Sasa, in *Proceedings of the 19th International Conference on the Physics of Semiconductors*, edited by W. Zawadzki (Polish Academy of Science, Warsaw, 1988), p. 55; H. Hirai and S. Komiyama, Phys. Rev. B **40**, 7767 (1989); H. Hirai, S. Komiyama, S. Sasa, and T. Fujii, J. Phys. Soc. Jpn. **58**, 4086 (1989).
- ³⁸R. J. Haug, A. H. MacDonald, P. Streda, and K. von Klitzing, Phys. Rev. Lett. **61**, 2797 (1988).
- ³⁹S. Washburn, A. B. Fowler, H. Schmid, and D. Kern, Phys. Rev. Lett. **61**, 2801 (1988).
- ⁴⁰B. W. Alphenaar, P. L. MacEuen, R. G. Wheeler, and R. N. Sacks, Phys. Rev. Lett. **64**, 677 (1990).
- ⁴¹D. B. Chklovskii, B. I. Shklovskii, and L. I. Glazman, Phys. Rev. B **46**, 4026 (1992).
- ⁴²D. B. Chklovskii, K. A. Matveev, and B. I. Shklovskii, Phys. Rev. B **47**, 12 605 (1993).
- ⁴³T. Suzuki and T. Ando, J. Phys. Soc. Jpn. **62**, 2986 (1993).
- ⁴⁴See, for example, C. W. J. Beenakker and H. van Houten, Solid State Phys. **44**, 1 (1991), and references cited therein, for the ballistic transport.
- ⁴⁵T. Ando, J. Phys. Soc. Jpn. **55**, 3199 (1986).
- ⁴⁶S. Hikami, Phys. Rev. B **29**, 3726 (1984); Prog. Theor. Phys. **72**, 722 (1984); **76**, 1210 (1986); **77**, 602 (1987).
- ⁴⁷S. Koch, R. J. Haug, K. von Klitzing, and K. Ploog, Phys. Rev. Lett. **67**, 883 (1991).